New iron tetrazolate frameworks: synthesis, temperature effect, thermal behaviour, Mössbauer and magnetic studies

Vanessa Pimenta, Quang Hoang Hanh Le, Lucy Clark, Jérôme Lhoste, Annie Hémon-Ribaud, Marc Leblanc, Jean-Marc Greneche, Gilles Dujardin, Philip Lightfoot, Vincent Maisonneuve

New iron tetrazolate frameworks: synthesis temperature effect, thermal behavior, Mössbauer and magnetic studies

Vanessa Pimenta,[a] Quang Hoang Hanh Le,[a] Lucy Clark,[b] Jérôme Lhoste,[a,*] Annie Hémon-Ribaud,[a] Marc Leblanc,[a] Jean-Marc Grenèche,[a] Gilles Dujardin,[a] Philip Lightfoot[b] and Vincent Maisonneuve.[a]

[a]*IMMM-UMR 6283 CNRS, LUNAM, Faculté des Sciences et Techniques, Université du Maine, Avenue Olivier Messiaen, 72085 Le Mans Cedex 9, France*
[b]*School of Chemistry and EaStChem, University of St. Andrews, St. Andrews, Fife, KY16 9ST, United Kingdom*

[*] To whom correspondence should be addressed. E-mail: jerome.lhoste@univ-lemans.fr
Phone: (33).(0)2 43 83 33 59. Fax: (33).(0)2 43 83 35 06

SUPPLEMENTARY INFORMATION

Table S1. Atomic coordinates and equivalent ADP of [H*dma*]·($Fe_5F_8(H_2O)_2$(*amtetraz*)$_4$) (1)

Atom	Wyckoff position	τ	x	y	z	B_{eq}(Å^2)
Fe(1)	1d	1	½	0	0	3,34(8)
Fe(2)	1a	1	0	0	0	3,24(8)
Fe(3)	2l	1	½	0.36593(9)	½	1,83(3)
Fe(4)	1f	1	0	½	½	2,16(5)
F(1)	2m	1	0.190(2)	0	-0.1361(7)	3,1(2)
F(2)	4o	1	0.2041(9)	0.3842(4)	0.5206(12)	5,1(2)
F(3)/OW(3)	2n	0.5/0.5	0.587(2)	½	0.6606(9)	3,5(2)
F(4)/OW(4)	2n	0.5/0.5	0.044(2)	½	0.7241(12)	5,9(4)
N(1)	4o	1	0.209(2)	0.1248(7)	0.1406(12)	4,3(4)
N(2)	4o	1	0.418(2)	0.1234(7)	0.1468(10)	4,7(3)
N(3)	4o	1	0.522(2)	0.1964(7)	0.2489(11)	4,3(3)
N(4)	4o	1	0.399(2)	0.2479(4)	0.3127(8)	3,6(2)
N(5)	4o	1	-0.0029(16)	0.2336(8)	0.2700(16)	5,6(3)
C(1)	4o	1	0.204(2)	0.2018(8)	0.2425(12)	3,9(3)
C(1)A	2j	0.5	½	0.401(3)	0	3,5(6)
N(1)A	2n	0.25	0.457(8)	½	-0.107(6)	2,8(9)
C(2)A	2m	0.50	0.185(3)	0	-0.503(4)	2,1(3)
N(2)A	4o	0.125	0.003(11)	0.044(4)	-0.446(6)	2,4(9)

Table S2. Atomic coordinates and equivalent ADP of [H*dma*]$_{1.5}$·($Fe_5F_7(H_2O)$(HCOO)(*amtetraz*)$_4$) (2)

Atom	Wyckoff position	τ	x	y	z	B_{eq}(Å^2)
Fe(1)	1d	1	½	0	0	1,24(2)
Fe(2)	1a	1	0	0	0	1,11(2)
Fe(3)	2l	1	½	0.36653(6)	½	1,29(2)
Fe(4)	1f	1	0	½	½	1,46(2)
F(1)	2m	1	0.8042(5)	0	0.1388(4)	1,76(6)
F(2)	4o	1	0.2183(4)	0.38055(18)	0.5425(3)	2,16(4)
F(3)/OW(3)	2n	0.25/0.75	0.6061(6)	½	0.6660(5)	2,03(6)
F(4)/OW(4)	2n	0.25/0.75	-0.0035(8)	½	0.2577(5)	3,53(9)
N(1)	4o	1	0.7972(5)	0.1250(3)	0.8589(4)	1,64(6)
N(2)	4o	1	0.5890(5)	0.1212(3)	0.8501(4)	1,65(6)
N(3)	4o	1	0.4812(5)	0.1927(3)	0.7506(4)	1,84(6)
N(4)	4o	1	0.6162(5)	0.2471(3)	0.6892(4)	1,60(6)
C(1)	4o	1	0.8082(6)	0.2050(3)	0.7593(5)	1,76(6)
N(5)	4o	1	0.9897(6)	0.2360(4)	0.7306(6)	4,1(2)
C(4)	2n	0.50	0.176(2)	½	0.2290(18)	3,4(3)
C(1)A	2j	0.75	½	0.4010(7)	0	3,9(3)
N(1)A	2n	0.375	0.437(2)	½	0.9086(17)	2,8(3)
C(2)A	2m	0.75	-0.1875(16)	0	0.5031(11)	3,6(3)
N(2)A	4o	0.1875	-0.050(4)	-0.0477(18)	0.460(2)	3,5(5)

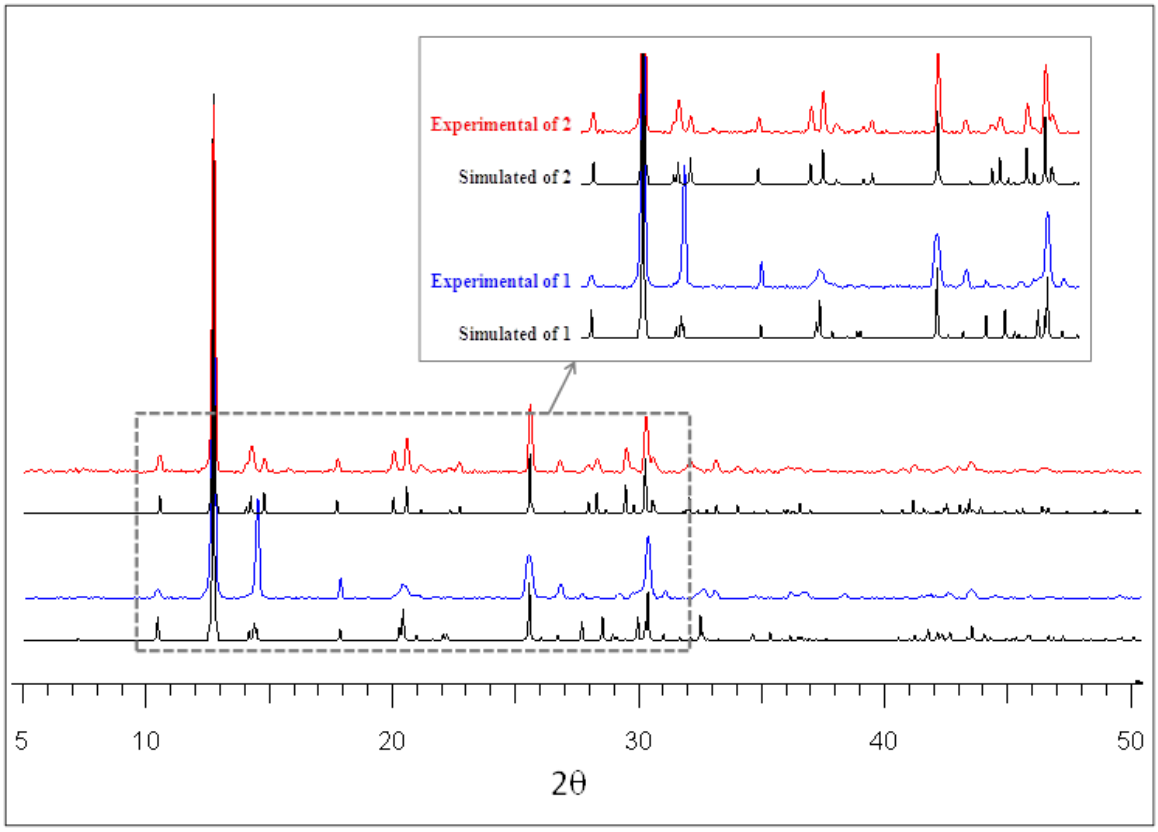

Figure S1. Experimental and simulated XRD patterns of [H*dma*]·($Fe_5F_8(H_2O)_2$(*amtetraz*)$_4$) (1) and [H*dma*]$_{1.5}$·($Fe_5F_7(H_2O)(HCOO)$(*amtetraz*)$_4$) (2)

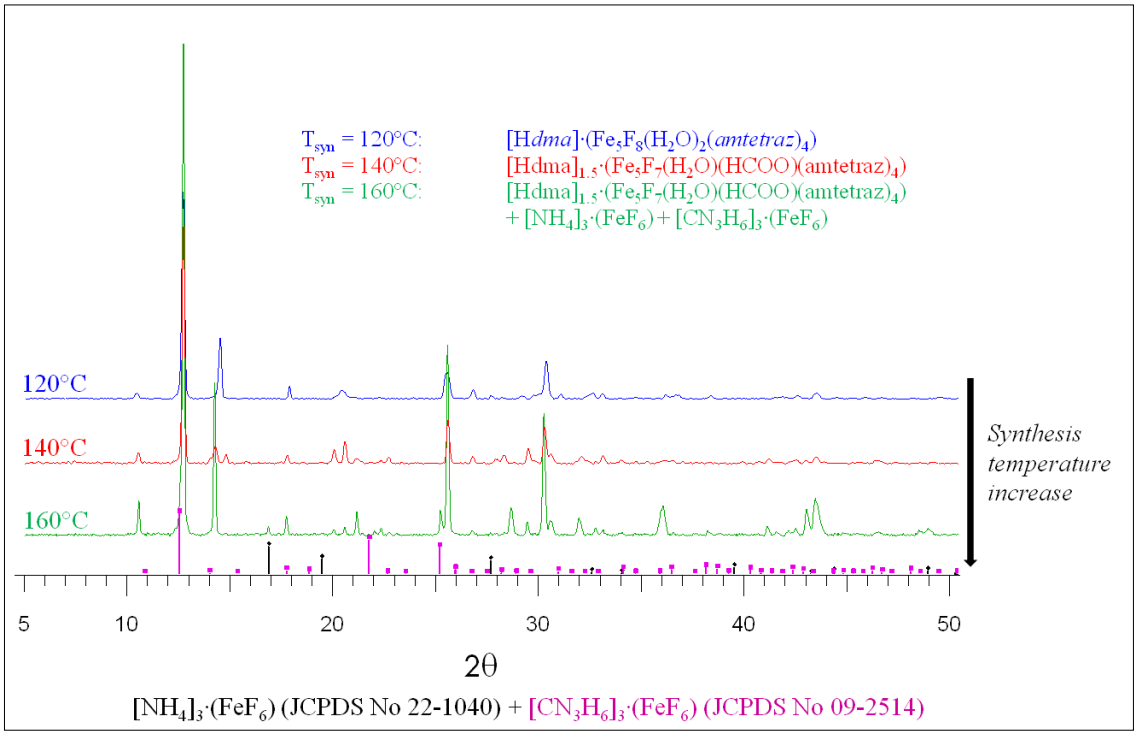

Figure S2. Evolution of XRD patterns and phase composition as a function of the synthesis temperature

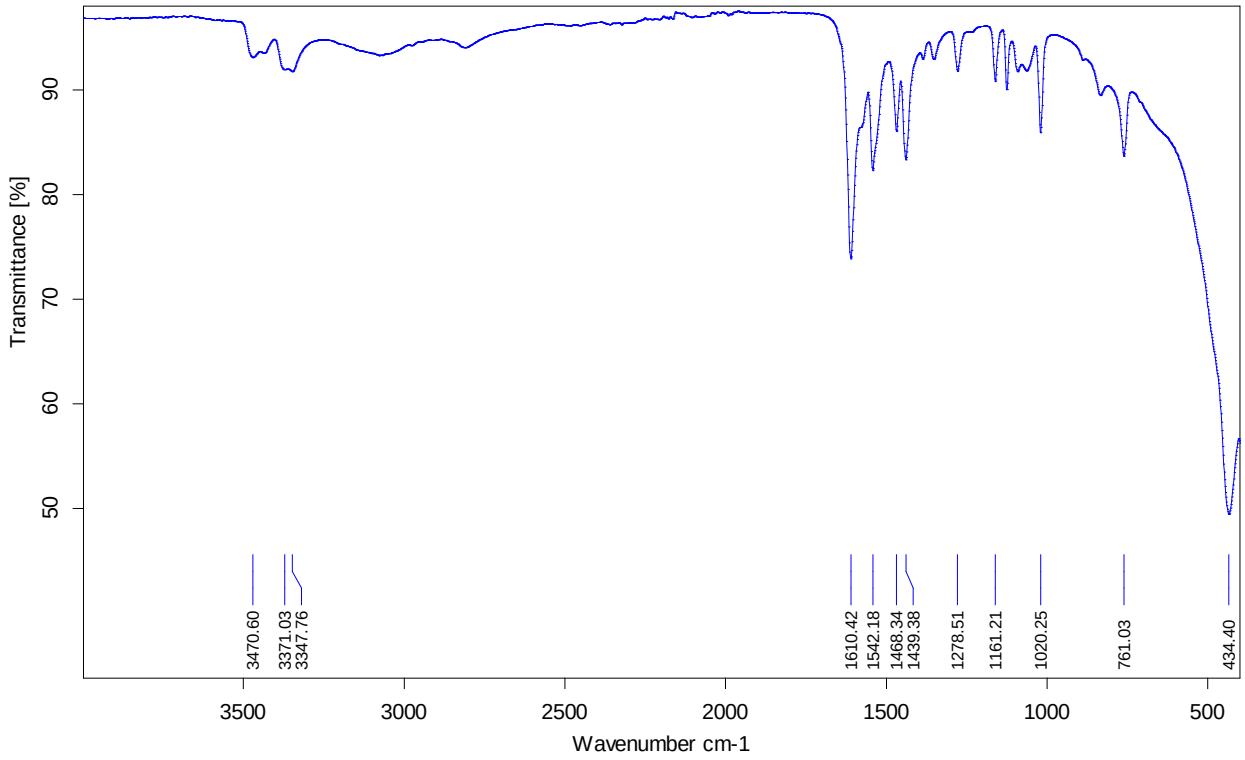

Figure S3. Infrared spectroscopy of [H*dma*]·($Fe_5F_8(H_2O)_2$(*amtetraz*)$_4$) (1)

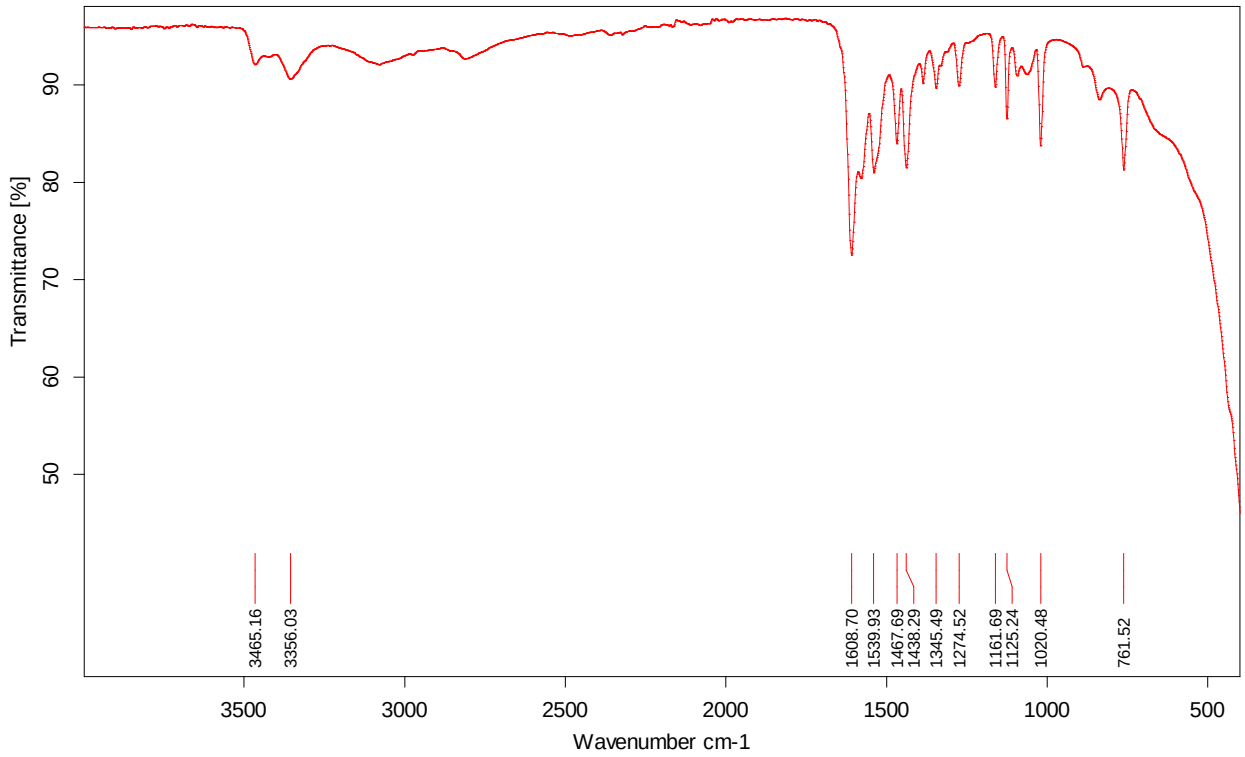

Figure S4. Infrared spectroscopy of [Hdma]$_{1.5}$·($Fe_5F_7(H_2O)$(HCOO)(*amtetraz*)$_4$) (2)